euspen's 23rd International Conference & Exhibition, Copenhagen, DK, June 2023
www.euspen.eu

# A method for developing predictive models of quality metrics and gas flow variables for 316L PBF-LB/M printed components based on image analysis

L.N. Frandsen[1], C.K. Kristensen[1], L. Haahr-Lillevang[2], C.G. Klingaa[2], S. Mohanty[3], M.M. Pedersen[1]

[1]*Department of Mechanical and Production Engineering, Aarhus University, Katrinebjergvej 89 G-F, 8200 Aarhus N, Denmark*
[2]*Center for Industrial 3D-printing, Danish Technological Institute, Kongsvang Allé 29, 8000 Aarhus C, Denmark*
[3]*Department of Mechanical Engineering, Technical University of Denmark, Produktionstorvet, Building 425, 2800 Kgs. Lyngby, Denmark*

*Lunifra@gmail.com*

**Abstract**
Powder bed fusion of metals by a laser beam (PBF-LB/M) is more commonly used than ever in a commercial setting. This requires more focus on product quality, homogeneity, and reproducibility. To obtain this, fast predictive models can be used. These models can give an indication of the approximate properties of the products before they are finished. This study aimed to develop predictive models for selected quality metrics and gas flow variables. The models were developed by analysis of images captured during a build of PBF-LB/M printed components in 316L stainless steel. The images were corrected for lighting inconsistencies followed by component-wise quantification of mean pixel intensity which formed the basis for the predictive models generated using JMP Pro 16. Response screening analyses were done to identify significant correlations between quantification methods and quality metrics or gas flow variables. A correlation between the quality metric bulk $O_2$, which is the oxygen uptake in the bulk material, and the quantification method "mean value bulk" was found. Additionally, a correlation between the gas flow variable oxygen percentage in the build chamber and the "mean value circular" quantification method was found. Thus, two predictive models were developed. The model for bulk $O_2$ could not be validated as further data processing was needed for the remaining components used for validation. This was mainly due to time and equipment limitations. The oxygen percentage model was tested but seemed unusable as the predictions were inaccurate. This result is likely caused by depositions of process by-products on the surface of the studied components.

Laser powder bed fusion, Additive manufacturing, Design of experiments, Predictive modelling

## 1. Introduction

Powder bed fusion of metals by a laser beam (PBF-LB/M) is a technique and an additive manufacturing process that allows three-dimensional manufacturing. PBF-LB/M is used today for both rapid prototyping, but also to produce complex objects and is utilised in both research and industrial contexts. This setting requires more focus on product quality, homogeneity, and reproducibility.

As with any other technology, PBF-LB/M has its disadvantages. The process parameters regarding laser power and the protective gas atmosphere greatly influence the quality of components in relation to mechanical properties, tolerances, and visual appearance, and variations in these can lead to a critical failure of the components [1, 2]. To better control these process parameters, the development of predictive models is becoming increasingly important. A predictive model can predict the outcome, e.g., a mechanical property, when given the correct input.

The influence of gas flow variables (oxygen percentage, gas flow speed and relative pressure) on the quality metrics (internal channel roughness, bulk porosity, average channel diameter, equivalent diameter corresponding to the unobstructed cross-sectional area of the channel and the bulk hardness) in 316L stainless steel components were investigated by Klingaa *et al.* [3]. This was done using an SLM 280 PBF-LB/M system. The correlations found were used for the development of predictive models of the quality metrics.

Using quality metrics in predictive models is important because of the potential for in-situ control of the process parameters thereby increasing the probability of obtaining the desired as-built mechanical properties. The gas flow variables can potentially be used for sensor validation and can be implemented in a monitoring system warning the user if a parameter drift occurs. Overall, these measures could possibly reduce the number of failed builds, resulting in less waste of materials and energy. Additionally, the time spent testing for mechanical weaknesses and post-processing could likely be reduced by the prediction of mechanical properties and thus ensuring operation in the optimal parameter range.

This study aimed to investigate the same quality metrics as Klingaa *et al*. [3] plus one additional, the bulk oxygen uptake, and the gas flow variables through image analysis. This was done with the greyscale image data obtained by Klingaa *et al*. [3] from the embedded camera in the SLM 280 PBF-LB/M system. Correlations based on image data were then used for producing simple predictive models.

## 2. Methodology

The method used is composed of four steps.
1) Correction for lightning inconsistencies.
2) Separation of regions of interest from the background.
3) Quantification of the images.
4) Creation of simple predictive models.

The methodology was applied to images of test samples designed for the purpose. These were called components.

The components were designed in 316L stainless steel by Klingaa *et al. [3]* to test the selected quality metrics. This was done by altering the gas flow variables randomly for each component. The composition of a component can be seen in figure 1.

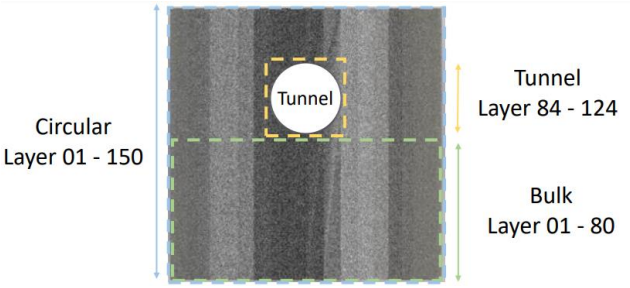


**Figure 1.** Design of a component marked with the three regions of interest marked by the blue, yellow and green dotted lines. (Sideways view)

The components were printed on top of each other and separated by 4 mm of support material. The components could be further categorized into towers. A tower consisted of 20 components. Four towers were printed in four different locations on the build platform as seen in figure 2.

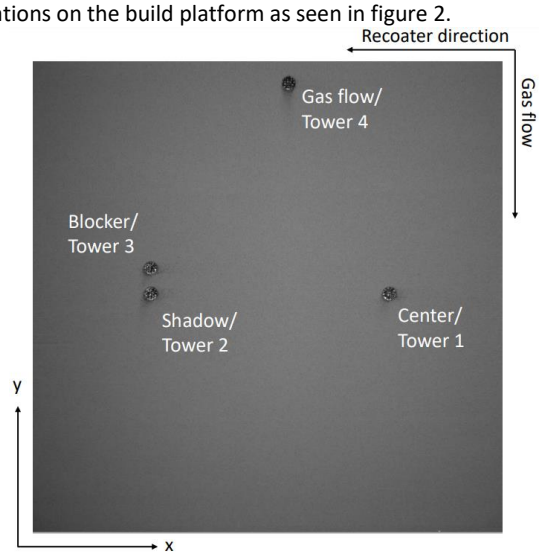


**Figure 2.** Tower placement on the build platform. (Top view)

### *2.1. Image correction*

First, the images were corrected because the image-to-image lighting changed randomly. The correction aimed to create even lighting throughout the build platform, as the edges appeared darker than the centre. This phenomenon is known as vignetting and can be seen in figure 2. The image correction was based on the colour of the background. The towers were overlayed with the mean intensity of the adjacent pixels. The images were then divided into 20x20 grids, and the mean value for each grid square was calculated. The correction was calculated with a target background light intensity of 127.5 as:

$$C_n = 127.5 - \bar{G}_n \tag{1}$$

Where $C_n$ is the correction applied to all pixels in the grid square $n$, $\bar{G}_n$ is the mean pixel intensity of the grid square $n$ and $n$ is the grid square number running from 1 to 400. The towers were then reinserted, and the correction was applied on every grid square. The correction resulted in an expansion of the intensity scale from 0 – 255 to -127.5 – 382.5.

### *2.2. Background separation*

A component contained three regions of interest (ROI), which were studied. To get the desired ROI, a combination of masks and layers was used. The layers containing the ROI can be seen in figure 1 and the masks can be seen in figure 3.

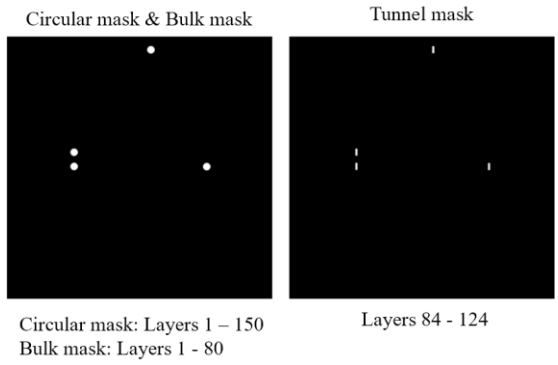


**Figure 3.** The different mask types used on images depending on ROI. (Top view)

The masks were overlayed on the images thereby removing all but the white-coloured pixel. This resulted in the components being separated from the background.

### *2.3. Image quantification*

The image quantification was a two-step process. First, the mean pixel intensity was observed for each component, then the components were binned.

### *2.4. Mean pixel intensity*

The mean pixel intensity was obtained with an in-house Python code by stacking all the image layers needed for the desired ROI. The mean pixel intensity was then calculated as:

$$\bar{I}(x,y) = \frac{\sum_{L=1}^{L} I(x,y)_L}{L} \tag{2}$$

Where $L$ is the number of layers in the ROI studied. $I$ is the intensity and $x$ and $y$ are the pixel coordinates. Iteration through all relevant $x$ and $y$ positions resulted in a mean light intensity component.

### *2.5. Binnig of data*

Each mean light intensity component was binned once it was calculated. The binning was considered necessary as the image data were inhomogeneous and exposed to sources of error. The Python code assigned each of the 20 mean light intensity components to a bin. The bin size was five which gave intervals going from 0 to 102. The binned data were both exported to JMP Pro and plotted. This plot is seen in figure 5.

### *2.6. Predictive models*

The predictive models were created using JMP Pro. First, the potential correlations were identified. This was done with the JMP response screening analysis, which took each possible pair of responses and factors and checked the correlation by a significance test with a selected significance level of 5%. The correlations were divided into two groups (1) the correlations between pixel intensity and the three gas flow variables; oxygen percentage, gas flow speed, and pressure, and (2) the correlations between pixel intensity and the quality metrics porosity, surface roughness, average diameter, equivalent diameter, hardness, and bulk $O_2$ uptake.

The grouping was done as the correlation between pixel intensity and the gas flow variables were interesting to

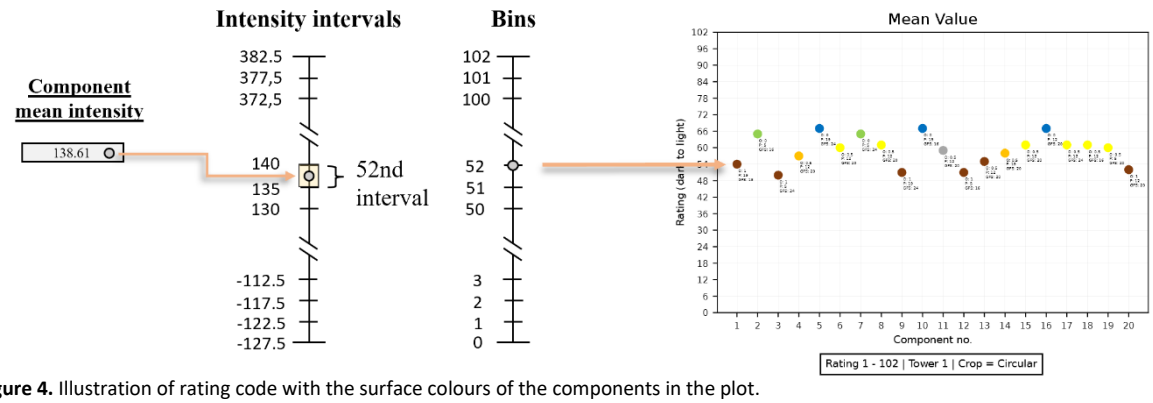


**Figure 4.** Illustration of rating code with the surface colours of the components in the plot.

investigate because these variables were identical for every set of components in all towers. This made validation across tower positions possible by basing the model on the best-positioned tower regarding gas flow and lighting, namely Tower 1, and then using the model to estimate the gas flow variables in the remaining tower positions (2, 3 and 4). The correlations for quality metrics could only be investigated for Tower 1, as the other towers had not been analysed.

Predictive models were created using real values with the JMP function "Fit model". The gas flow variable and quality metric were assigned as the response and the mean pixel intensity for each ROI was set as the factor. Both the main effect and the interaction of the factor were included. Non-significant terms were removed, and final models were created.

## 3. Results

A correlation between oxygen percentage in the build chamber and the quantification method "mean value circular", which is the mean pixel intensity for the circular ROI, was found. Furthermore, a correlation between bulk $O_2$, and the quantification method "mean value bulk", which is the mean pixel intensity for the bulk ROI, was found. Thus, two predictive models were developed. The predictive formula for oxygen percentage is:

$$O(MVC) = -0.045531687 \cdot MVC + 3.2101893314 \qquad (3)$$

Where MVC is the observed mean pixel intensity value for the circular ROI. The predictive formula for bulk oxygen percentage is:

$$Bulk\ O_2(MVB) = -0.000883533 \cdot MVB + 0.0922218097 \qquad (4)$$

Where MVB is the observed mean pixel intensity value for the bulk ROI.

The oxygen level was predicted for the remaining towers and the mean residuals were calculated as the actual values minus the predicted value. These can be seen in table 1.

**Table 1** Mean residuals for oxygen prediction.

| Mean residuals – Oxygen model | | | |
|---|---|---|---|
| Tower 1 | Tower 2 | Tower 3 | Tower 4 |
| 0.02 | -0.15 | -0.24 | -0.68 |

The prediction residual for Tower 1 is near 0. The residuals for the remaining towers are negative. A negative residual means that the model predicts higher oxygen levels than anticipated.

## 4. Discussion

Even though the deviation of the residuals, in table 1, seems to be systematic this may not be the case. It can be hypothesised that the deviation is a result of process by-products, as dark-coloured by-products from the laser scanning could be deposited onto the components and reduce the pixel intensity. Further, the amount of deposition varies with tower position. Tower 1 is the only tower not affected by spatter depositions. Towers 2 and 3 could affect each other, with Tower 2 being scanned first and thereby depositing spatter particles and by-products on Tower 3, which is then included in the bulk once scanned. This is illustrated in figure 6.

It can be observed from the work of Repossini *et al. [4]* that spatter particles may travel up to 10 mm against the gas flow direction while using default scanning parameters. When scanning at lower laser power, the same is seen by Bidare *et al.* [5]. Towers 3 and 4 are positioned 7.5 mm apart, which makes the spatter deposition plausible. Further, this effect can be reinforced by by-product clouds resulting in lower laser energy densities because of beam attenuation.

Tower 4 is placed next to the gas inlet, which is a region known for bad gas flow. The gas flow is individual for every PBF-LB/M system. Still, Schniedenharn *et al.* [6] visualized for a laboratory

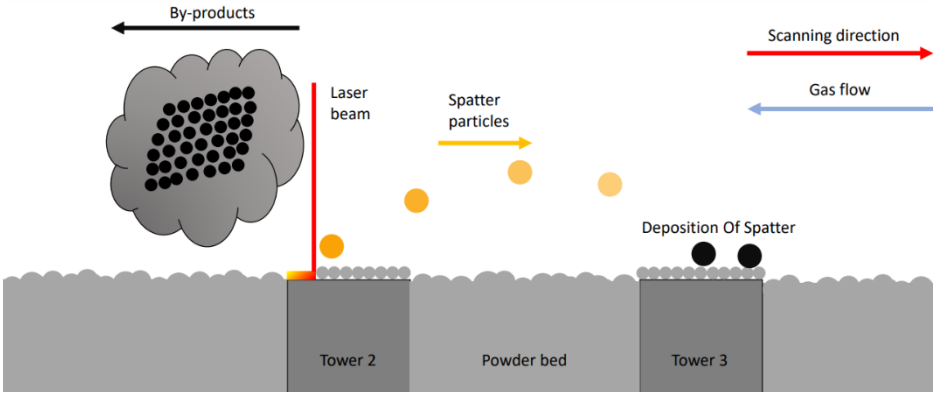


**Figure 5.** Spatter depositions on Tower 3.

machine the gas flow velocity profiles which showed an uneven velocity distribution in both the x and y direction, especially around the inlet. A fair assumption is that the gas flow is more turbulent at the inlet, where Tower 4 is positioned. By-products and spatter from Tower 4 could be projected into the air and redeposited on Tower 4 because of insufficient gas flow, as illustrated in figure 7.

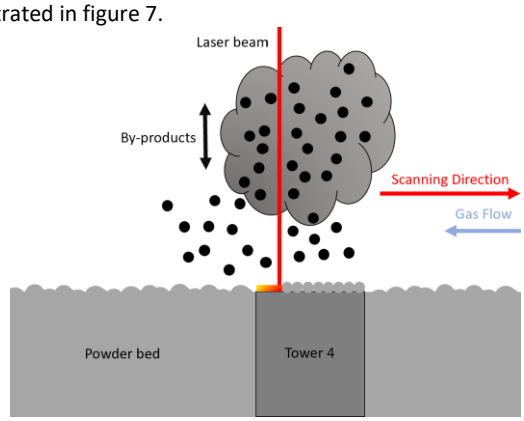


**Figure 6.** Depositions of by-products on Tower 4

If the hypothesis holds true, then the model from equation 2 is a bad descriptor for oxygen. In that case, the model does not describe oxygen content as intended but rather spatter and by-product depositions. The problem occurs because oxygen influences both the pixel intensities and spatter. According to Du Plessis *et al.* [2] a correlation between oxygen and surface colour exists, which is expressed as different pixel intensities. Oxygen is also a cause of spatter, as shown by Liu *et al.* [7]. This result makes the oxygen model obsolete and is likely the reason for the result in table 1.

The bulk $O_2$ model could, contrary to the oxygen model, be a reasonable descriptor of oxygen bulk uptake. This is because Deng *et al.* [8] showed that increased spatter inclusions resulted in a higher oxygen uptake, which resulted in lack-of-fusion defects and bad tolerances. Therefore, in typical use cases, it is desirable to reduce bulk $O_2$. If the stated hypothesis is true, it would be expected to see the highest number of spatter inclusions and bulk $O_2$ in Tower 4 followed by 3, 2 and 1.

In general, it seems that the image analysis predicts the amount of spatter deposited on the components. The surface oxidation of spatter particles was investigated by Simonelli *et al. [9].* The spatter surface consisted mainly of oxides from volatile elements of 316L. Oxides are hard and brittle and may influence the hardness, ductility, and strength of the components, despite no correlations found in this study. These effects can either be critical or desired depending on the product manufactured.

The predictive models were chosen to be simple. The advantage of doing this rather than relying on simulation-based evaluation is the computation time. This is favoured when doing an in-situ evaluation, as more demanding methods could slow the PBF-LB/M process.

## 5. Conclusion

From the study, the following conclusions can be drawn. There are strong correlations between:

- Oxygen and mean value circular
- Bulk $O_2$ and mean value bulk

The correlations were utilised in simple predictive models, which have been created, and the results examined. The results showed an error for the oxygen model related to tower position, probably due to by-product and spatter depositions. The oxygen model and its results are of no importance, but the method for creating this can still be applied to other builds, materials or PBF-LB/M systems.

The model regarding bulk $O_2$ and mean value bulk is likely more applicable, but final data processing for the remaining towers and subsequent model validation is still needed. This correlation is important as higher oxygen uptake can affect the quality of the components. The work described was done with the developed quantification and image analysis techniques. The results showed potential for further development in the field of image analysis with embedded cameras of PBF-LB/M printed components to predict print parameters.

This study allows for future work. The model can only predict bulk $O_2$, but this should be implemented in a feedback loop to fully utilise the capabilities, sending information about parameter correction to the PBF-LB/M system in situ. For this to happen, further studies need to be done to investigate the relationship between Bulk O2 and other traditional PBF-LB/M parameters such as scanning speed, laser power etc. Further, as spatter seems to have a significant impact on the pixel intensities observed, further studies could be made to control the spatter deposition on neighbouring parts. This could result in an autonomous system calculating either ideal part placement or gas flow to reduce the amount of spatter deposited from adjacent parts, as seen in Towers 2 and 3 and self-deposition, as seen in Tower 4. Also, understanding the full effect of large spatter depositions regarding oxide inclusions and the effect on hardness, ductility, and strength could be interesting and could have implications for the future of spatter deposition and image analysis.

## References

[1] Sefene E M 2022 State-of-the-art of selective laser melting process: A comprehensive review *Journal of Manufacturing Systems* **63** 250-74.

[2] Du Plessis A, MacDonald E, Waller J M and Berto F. 10 - Non-destructive testing of parts produced by laser powder bed fusion. In: Yadroitsev I, Yadroitsava I, du Plessis A, MacDonald E, editors. Fundamentals of Laser Powder Bed Fusion of Metals. (Amsterdam): (Elsevier); 2021. p. 277-300.

[3] Klingaa C G, Mohanty S, Funch C V, Hjermitslev A B, Haahr-Lillevang L and Hattel J H 2021 Towards a digital twin of laser powder bed fusion with a focus on gas flow variables *Journal of Manufacturing Processes* **65** 312-27.

[4] Repossini G, Laguzza V, Grasso M and Colosimo B M 2017 On the use of spatter signature for in-situ monitoring of Laser Powder Bed Fusion *Additive Manufacturing* **16** 35-48.

[5] Bidare P, Bitharas I, Ward R M, Attallah M M and Moore A J 2018 Fluid and particle dynamics in laser powder bed fusion *Acta Materialia* **142** 107-20.

[6] Schniedenharn M, Wiedemann F and Schleifenbaum J H 2018 Visualization of the shielding gas flow in SLM machines by space-resolved thermal anemometry *Rapid Prototyping Journal* **24**(8) 1296-304.

[7] Liu Y, Yang Y, Mai S, Wang D and Song C 2015 Investigation into spatter behavior during selective laser melting of AISI 316L stainless steel powder *Materials & Design* **87** 797-806.

[8] Deng P, Karadge M, Rebak R B, Gupta V K, Prorok B C and Lou X 2020 The origin and formation of oxygen inclusions in austenitic stainless steels manufactured by laser powder bed fusion *Additive Manufacturing* **35** 101334.

[9] Simonelli M, Tuck C, Aboulkhair N T, Maskery I, Ashcroft I, Wildman R D and Hague R 2015 A Study on the Laser Spatter and the Oxidation Reactions During Selective Laser Melting of 316L Stainless Steel, Al-Si10-Mg, and Ti-6Al-4V *Metallurgical and Materials Transactions A* **46**(9) 3842-51.